

---

# Soft projectile impacts analysis on thin reinforced concrete slabs: Tests, modelling and simulations

**C. Pontiroli\***, **A. Rouquand\***, **L. Daudeville\*\***, **J. Baroth\*\***

\* CEA, DAM, GRAMAT, F-46500 Gramat, France  
{christophe.pontiroli, alain.rouquand}@cea.fr

\*\* Université Joseph Fourier – Grenoble 1 / Grenoble INP / CNRS  
3SR Lab, Grenoble, F 38041, France  
jbaroth@ujf-grenoble.fr

---

*ABSTRACT. Numerical simulations of reinforced concrete structures subjected to high velocity impacts and explosions remain a difficult task today. Since ten years and more now, the CEA-Gramat has maintained a continuous research effort with the help of different French universities in order to overcome encountered difficulties in modeling the behavior of concrete structures under severe loading. To get more data on aircraft impact problems and then validate numerical models, soft projectile impacts tests at small scale on thin reinforced concrete slabs has been carried out at CEA-Gramat. Numerical simulations of these tests have been carried out and compared with experimental results to validate our numerical approach.*

*RÉSUMÉ. La simulation numérique de structures en béton armé soumises à des impacts à grande vitesse et à de fortes explosions reste encore aujourd'hui une tâche difficile. Depuis plus de dix ans, le CEA-Gramat poursuit un programme de recherche, avec la participation de plusieurs laboratoires universitaires français, afin de lever les difficultés associées à la modélisation du comportement des structures en béton sous chargement extrême. Pour acquérir des données sur la tenue de structures aux impacts d'avions et ainsi pouvoir valider les outils numériques qu'il développe, le CEA-Gramat a réalisé un certain nombre de tests expérimentaux d'impacts de projectiles déformables sur des dalles en béton armé peu épaisses. Les simulations numériques de ces essais ont été réalisées et comparées aux résultats expérimentaux afin de valider les outils numériques mis en place au CEA-Gramat.*

*KEYWORDS: Impact, experiment, concrete model, simulation*

*MOTS-CLÉS: Impact, expérimentations, modèle de comportement, béton, simulation*

---

## 1. Introduction

Reinforced concrete structures like nuclear plants have to withstand the impact of different types of projectiles. A lot of experimental work has been carried out for

military threats in the past to investigate the effect of rigid projectile impacts, but few results are available on the interaction between a concrete structure and a highly deformable projectile (Riech *et al.*, 1984).

Recently, CEA-Gramat has participated to the International benchmark called: IRIS 2010. This benchmark was co-organized by the French Institute of Radio Protection and Nuclear Safety (IRSN) and by the VTT Research Institute in Finland. Some results of this test were known and the participants could use these experimental data to optimize their numerical results. Others tests were performed by the VTT research center and the results were unknown (Saarenheimo *et al.*, 2007). The numerical simulations of these tests were blind simulations. Good results were on the whole obtained with CEA-Gramat on these simulations (Rouquand, 2010), but some data like material characteristics were insufficient and some assumptions have been made to perform the simulations.

In the framework of the French VULCAIN PGCU 2007 research project (founded by the French National Research Agency), CEA-Gramat has proposed to carry out impact tests on reinforced concrete slabs with deformable projectiles. Concrete and steel material used for slabs have been characterized to give material parameters to numerical models, and a specific experiment have been developed to characterize the projectile crushing.

Soft impact induces both local damage and overall global dynamic response of the target. As shown Figure 1 (Jonas W. *et al.*, 1982) local damage consists of several processes: In a first stage [Figure 1 (1) to (4)], the projectile crushes and creates cratering on the front face of the reinforced concrete slab. Some shear cracks are developed through the slab thickness and along the rear face reinforcement. In a second stage [Figure 1 (5) to (8)], these cracks propagate and then a plugging followed by a back face scabbing damage mode appear. If the projectile continues to push the plug, the rear reinforcements fail and the plug is completely sheared off: perforation is reached.

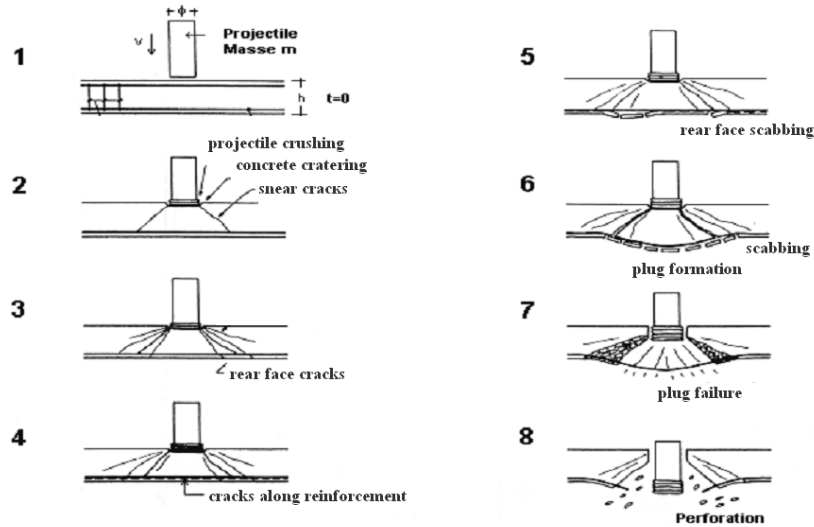


**Figure 1.** Successive steps of the process of soft impact on reinforced concrete slab (Jonas W. et al., 1982)

In this paper, new soft impact experiments are presented and the test results are compared with numerical simulations using the finite element method and a specific concrete material model.

## 2. Impact tests

### 2.1 Experimental procedures

A steel cylindrical projectile with sections of different thicknesses is launched on a target by a 90 mm caliber gas gun (Figure 2). Front part of the projectile is composed of a thin steel S235 tube ( $d=80$  mm,  $L=500$  mm). This tube has a thickness of 1 mm over the first 250 mm front part and a thickness of 2 mm on the remaining 250 mm part. The third and rear part of the projectile is composed of a massive steel 35NCD16 cylinder incorporating an acceleration recorder system designed to measure the axial accelerations during the tests.



**Figure 2.** Gas launcher, deformable projectile and target

Rectangular 2 m by 1.2 m reinforced concrete slabs with a thickness of 7 or 6 cm have been used to simulate soft projectile impact. The projectile velocity is changed in order to get different damage levels ranging from slight bending to projectile perforation.

The target is held tight by a metallic support which is supposed to be perfectly rigid. Video cameras and displacement sensors located on the rear face of the reinforced concrete slab complete the measurements. Nine tests have been performed with different impact velocities going from 70 to 135 m/s. In this paper we present two experimental results obtained on concrete slabs of 7 cm thick for velocities of 107.5 m/s (test n°1) and 70.2 m/s (test n°2). Other results are gathered in (Baroth *et al.*, 2011).

A complementary particular test has been designed to get information on the projectile crushing behavior. This experiment is a ballistic pendulum test which consists in measuring the projectile momentum, from which it is possible to calculate the velocity and the kinetic energy.

## **2.2 Concrete composition**

A standard concrete mixture named R30A7, defined several years ago by CEA-Gramat and 3SR Laboratory at Grenoble, is used with an amount of 1.0 vol. % steel reinforcement ( $d = 6$  mm S235 steel rebar with 80 x 80 mm square grid, rebar are located at 19 mm to the faces).

The tested R30A7 concrete displays a 28-day compressive strength of about 30 MPa and a slump of 7 cm. It should be noted that a very high-quality cement is used. This high quality gives better material reproducibility and leads to a particularly low cement volume. Aggregate compounds, with a maximum size of 8 mm are obtained from natural deposits (rolled aggregates, 99% quartzite). Table 1 gives the composition and the mechanical properties of the R30A7 concrete.

**Table 1.** *Composition and mechanical properties of the R30A7 concrete*

<i>Concrete composition</i>	<i>R30A7</i>
0.5/8 "D" gravel (kg/m <sup>3</sup> )	1008
1.800 μm "D" sand (kg/m <sup>3</sup> )	838
CEM I 52.5 N PM ES CP2 cement (Vicat) (kg/m <sup>3</sup> )	263
Water (kg/m <sup>3</sup> )	169
W/C ratio	0.64
Cement paste volume $V_p$ (m <sup>3</sup> /m <sup>3</sup> )	0.252
Density (kg/m <sup>3</sup> )	2278
<i>Mechanical properties</i>	
Average tested strength in uniaxial compression at 28 days (MPa)	32.5
Average slump measured using the Abrams cone (cm)	6.9
Volume of occluded air measured in fresh concrete (l/m <sup>3</sup> )	34
Porosity accessible to water (%)	12

### 2.3 Test results

#### 2.3.1 Perforation test

Test n°1, corresponding to an initial projectile velocity of 107.5 m/s, results in perforation of the reinforced concrete slab with a projectile residual velocity of about 46.6 m/s. A series of plies are formed on the steel tube during the projectile crushing process and the first cylinder part with a thin wall thickness of 1 mm is completely buckled (Figure 3).



**Figure 3.** *Deformation of the missile after perforation (test n°1,  $V_0 = 107.5$  m/s)*

Figure 4 shows the residual damage obtained on the front and on the rear faces of the reinforced concrete target. We can observe the formation of a plugging cone on the front face with an important scabbing effect on the rear face. Several rebars fail on the rear face.

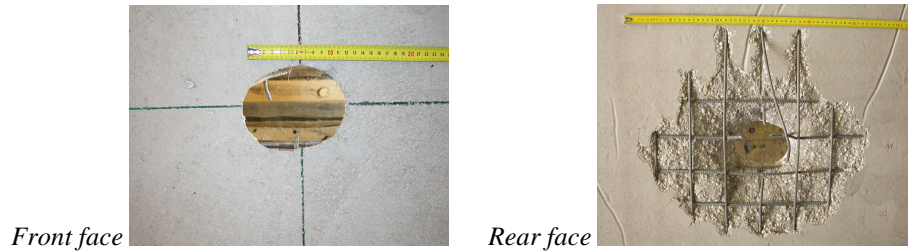


**Figure 4.** Damage of the reinforced concrete slab after test n°1 ( $V_0 = 107.5$  m/s)

### 2.3.2 Non perforating test

Test n°2 presented here (initial velocity of 70.2 m/s), results in a rebound of the projectile. A series of plies are formed on the steel tube during the projectile crushing process and the first cylinder part with a thin wall thickness of 1 mm is buckled over a length of 150 mm (Figure 5).



**Figure 5.** Deformation of the missile after perforation (test n°2,  $V_0 = 70.2$  m/s)

Figure 6 shows the damage obtained on the front and on the rear faces of the reinforced concrete target. We can observe scabbing effects and the formation of a plugging cone, but the failure of steel reinforcement is not reached. Kinetic energy of the projectile is not sufficient to perforate the reinforced concrete slab.

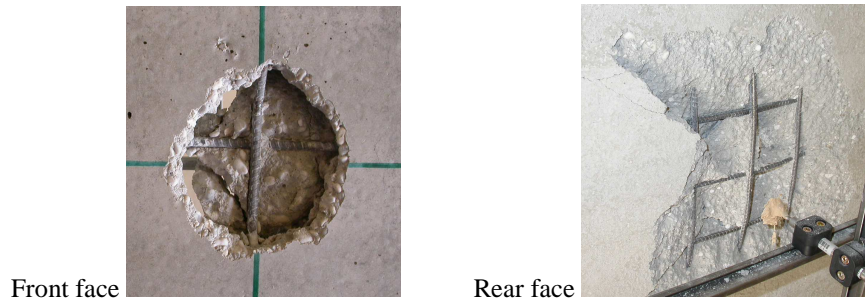


**Figure 6.** Damage on the reinforced concrete slab after test n°2,  $V_0 = 70.2$  m/s

### 2.3.4 Ballistic limit

Eight experimental tests have been performed on slabs with a thickness of 7 cm (see Table 2). As the projectiles haven't exactly the same mass, we give on Figure 7 the ballistic limit curve in terms of kinetic energy. Tests n°1 (#24) and n°2 (#32) are located on both sides of the ballistic limit which can be estimated around 92 m/s.

**Table 2.** Specific data concerning each of eight Vulcain tests (Baroth, 2011)

Reference	#22	#24	#30	#35	#27	#43	#32	#34
$M$ (kg)	6.166	5.207	5.091	5.059	4.985	5.050	5.065	5.059
$E_c$ (kJ)	56.6	29.8	21.5	13.5	21.6	16.2	12.4	11.7
$V$ (m/s)	135.5	107.5	92	73	93	80	70.2	68

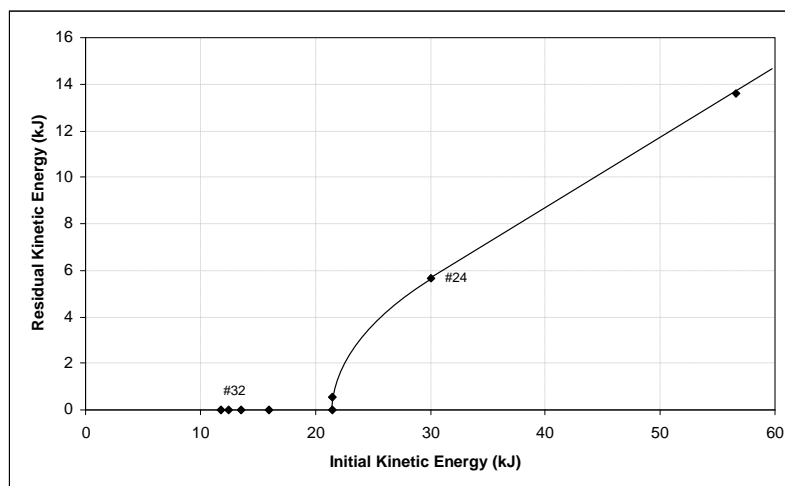


**Figure 7.** Ballistic limit curve for the experimental series with slabs 7 cm thick

2.3.3 Ballistic pendulum test

Numerical simulations of soft projectile impact on a reinforced concrete structure require a relevant concrete model but also a good modeling of the projectile crushing process. In order to get information on projectile deformation during soft impact and to validate the projectile material model and its data, a ballistic pendulum test is proposed. This test consists in launch a deformable projectile on a massive rigid body (weight of 153 kg) hung to the ceiling with two steel cables (Figure 8). During the projectile crushing phase the load is transferred to the rigid mass that is accelerated. The measurement in the early time of the displacement, velocity, and acceleration give the value of the applied load.

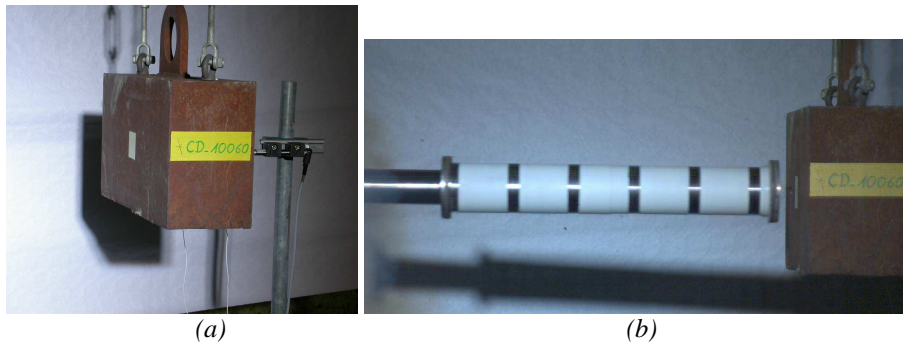


**Figure 8.** Ballistic pendulum device (a) and photo just before impact (b)

In this experiment, projectile has been launched with a striking velocity of 89.2 m/s. Figure 9 shows the residual shape of the projectile at the end of test. We can observe a series of regular plies formed on the steel tube. The projectile residual lengths have been measured:  $L_H = 215$  mm,  $I_H = 0$  mm,  $I_T = 38$  mm.

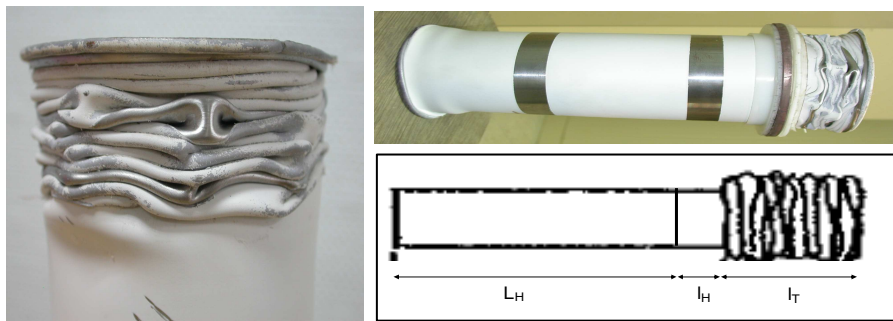


**Figure 9.** Projectile deformation after test ( $V_0 = 89.2$  m/s)

Using a displacement sensor located on the rear face of the steel block, the pendulum velocity can be obtained. During the first 5 ms, the pendulum is set in motion then the velocity reaches a constant value of about 3.2 m/s.

### 3. Numerical simulations

These tests have been simulated using the finite element method and a specific concrete material model which is presented hereafter.

#### 3.1 Damage model for concrete: PRM Model

A damage model has been developed at CEA-Gramat to simulate the behavior of concrete under severe loading (Pontiroli *et al.*, 2010). This model, named ‘‘PRM model’’, includes two scalar damage variables that give respectively the loss of stiffness under tensile loading  $D_t$  and the loss of stiffness under compressive loading  $D_c$  (see Figure 10). Between these two loading states a transition zone is defined by  $(\sigma_{ft}, \varepsilon_{ft})$  where  $\sigma_{ft}$  and  $\varepsilon_{ft}$  are the crack closure stress and the crack closure strain respectively. The main equations of the PRM model for a uniaxial loading are:

$$\text{for traction: } (\sigma - \sigma_{ft}) = E_0 (1 - D_t) \cdot (\varepsilon - \varepsilon_{ft})$$

$$\text{for compression: } (\sigma - \sigma_{ft}) = E_0 (1 - D_c) \cdot (\varepsilon - \varepsilon_{ft})$$

$E_0$  is the initial Young’s modulus and the damage evolution laws for  $D_t$  and  $D_c$  are controlled by an equivalent tensile strain (Mazars, 1984).

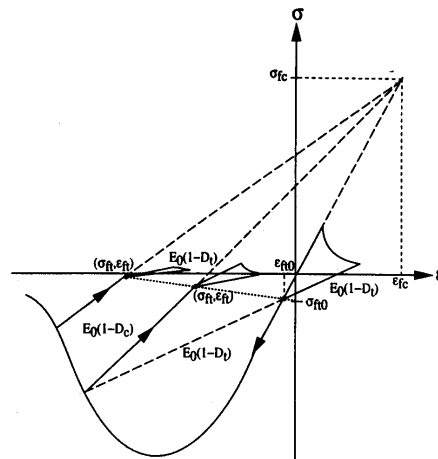


**Figure 10.** Stress strain curve for a tensile - compressive loading

Strain rate effects are introduced to model the increase of the maximum tensile stress observed under moderate and high strain rate loading. Experimental data have been obtained on the R30A7 concrete using the Hopkinson bar facility at LEM3 laboratory (Metz, France) and using an impulsive electromagnetic pressure generator device (GEPI) at CEA-Gramat (see Figure 11).

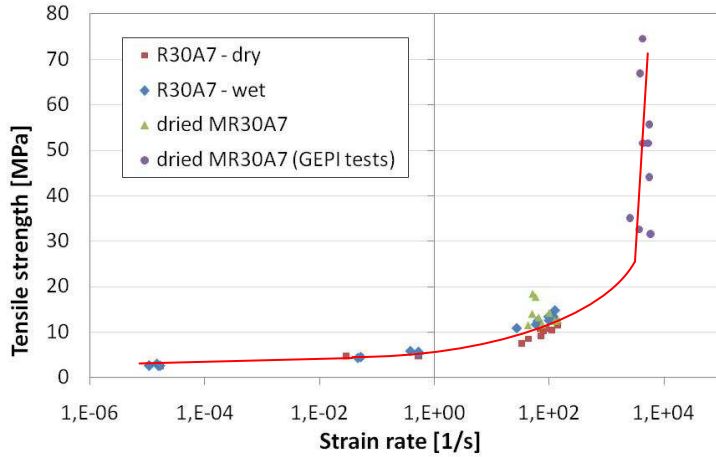


**Figure 11.** Experimental strain rate effects obtained on the R30A7 concrete (Erzar B. et al., 2009)

A frictional stress is also added to simulate hysteresis loops during unloading and reloading paths (Figure 12). These frictional stresses introduce internal damping forces which are frequency independent but are related to damage parameters and then to tensile cracking phenomena. This effect can be significant for structural bending response and is essential to reproduce correctly residual displacement.

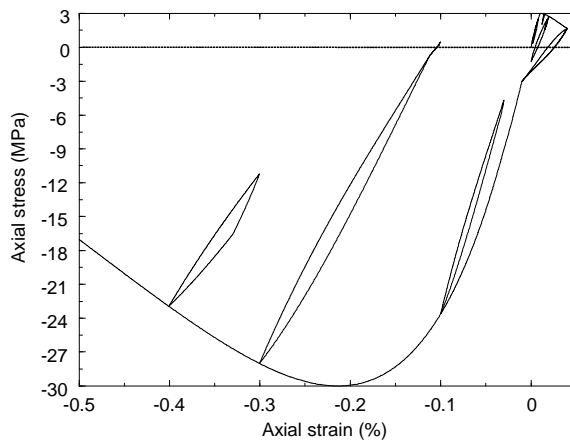


**Figure 12.** PRM damage model: cyclic loading including damping stresses

Under high pressure regime in porous material like concrete, irreversible shear strain can be observed like compaction and shear yield. These phenomena can drive a significant part of the material response (Gabet T. *et al.*, 2008), (Vu *et al.*, 2008). In order to take into account all these physical mechanisms, the plastic Krieg model has been coupled to the PRM damage model (Pontioli *et al.*, 2010).

But plasticity part of the PRM model has not been activated to simulate the soft impact tests carried out at CEA-Gramat. In our experiments the damage drives the concrete response and confinement pressure doesn't seem sufficient to play a significant role in the concrete behavior. Impact numerical simulations performed in this study have showed a maximum mean stress about 60-80 MPa in concrete.

The Hillerborg regularization concept (Hillerborg *et al.*, 1976) has been applied to limit mesh dependency during strain and damage localization phenomena.

The PRM model is available as a user subroutine (VUMAT) in the ABAQUS explicit finite element code. It is compatible with almost all the finite element library (1D truss elements, beam elements, 2D plane strain and plane stress elements, 2D axisymmetric elements, 3D solid elements).

### 3.2 Plastic model for steel rebar

The behavior of the steel reinforcement is simulated using the Johnson Cook dynamic failure model (Johnson G. R., 1985). This model allows for strain rate effect on the material strength but also on the material ductility (see Figure 13). For failure under high strain rates, these two effects must be taken into account to correctly reproduce material response.

In classical Johnson Cook model, the plastic stress  $\bar{\sigma}$  is related to the plastic strain  $\bar{\epsilon}^{pl}$ , to the plastic strain rate  $\dot{\bar{\epsilon}}^{pl}$  and to the damage variable  $D$  via the following expression:

$$\bar{\sigma} = (1 - D) \left[ A + B \left( \bar{\epsilon}^{pl} \right)^n \right] \left[ 1 + C \ln \left( \frac{\dot{\bar{\epsilon}}^{pl}}{\dot{\epsilon}_0} \right) \right]$$

$\dot{\epsilon}_0$  is a reference strain rate. A, B, n and C are material parameters.

The damage D is related to the plastic strain as follow:

$$D = \min \left( \frac{L_c \max \left( \sum_i \Delta \bar{\epsilon}_i^{pl} - \bar{\epsilon}^{pl0}, 0 \right)}{L_0 \bar{\epsilon}_f^{pl}}, 1 \right)$$

$\bar{\epsilon}^{pl0}$  is the plastic threshold. The damage variable D is incremented when the cumulated plastic strain  $\sum_i \Delta \bar{\epsilon}_i^{pl}$  becomes greater than the plastic threshold  $\bar{\epsilon}^{pl0}$ .

The plastic threshold  $\bar{\epsilon}^{pl0}$  is given by: 
$$\bar{\epsilon}^{pl0} = d_1 \left[ 1 + d_2 \ln \left( \frac{\dot{\bar{\epsilon}}^{pl}}{\dot{\bar{\epsilon}}_0} \right) \right]$$

$d_1$  and  $d_2$  are material parameters.  $L_e$  is the element characteristic length.  $L_0 \bar{\epsilon}_f^{pl}$  is the failure displacement.

Figure 13 shows stress strain curve obtained with the Johnson Cook dynamic failure model for S235 steel material used for rebar. We have the following material parameters: A = 480 MPa, B = 153 MPa, n = 0.36, C = 0.0141,  $d_1 = 0.045$ ,  $d_2 = 0.203$ ,  $L_0 = 0.2$

In this figure, the curves correspond to different constant strain rates given in the legend.

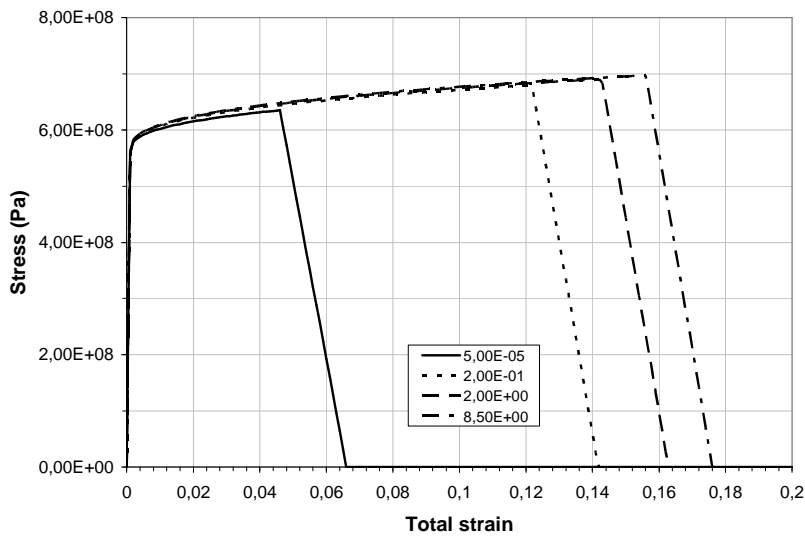


**Figure 13.** Example of a stress strain curve (Johnson Cook dynamic failure model), for different strain rates

### 3.3 Numerical results

Numerical simulations of soft impact tests are not easy because there are strong interactions between the target behavior and the projectile crash process. Correct predictions require a proper modeling of both the target and the missile response. In order to evaluate the capabilities of the explicit finite element code Abaqus including the PRM model, 3-D numerical simulations of CEA-Gramat impact tests have been undertaken. The objective is to determine the capabilities and the limits of such simulations.

#### 3.3.1 Ballistic pendulum simulation

First, to validate the deformable projectile model, the ballistic pendulum test has been simulated. The projectile is composed of a thin steel tube which is efficiently modeled using 3-D shell elements (1 568 elements). Eight nodes solid elements have been used for the massive steel block. 1D truss elements are used for the steel cables [Figure 14 (a)].

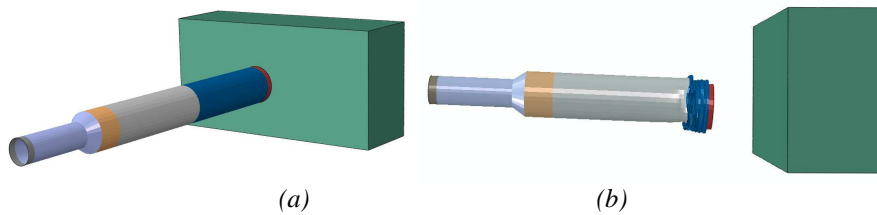


**Figure 14.** Ballistic pendulum simulation

The classical Johnson Cook model is used for projectile steel with the following material characteristics:  $A = 480$  MPa,  $B = 300$  MPa,  $C = 0.12$ ,  $n = 0.36$ . As experiments haven't showed failure on projectile, we haven't used dynamic failure option in Johnson Cook model.

The residual projectile shape shown on Figure 14 (b) gives a reasonably good approximation of the experimental result presented on Figure 9. Projectile residual lengths are in good agreement ( $I_T = 38$  mm) but the total number of plies is underestimated by the simulation (7 plies obtained numerically and 13 experimentally). The mesh of the projectile seems to be too coarse to reproduce correctly the plies formation during the crush.

On Figure 15, the projectile velocity (calculated by integration of the accelerometer signal) and the massive steel block velocity (calculated by derivation of the displacement signal) obtained during the experiment, are compared to the numerical results. The numerical simulation is able to reproduce the missile deceleration and the rebound at the end of the impact process. A good agreement is also obtained for the pendulum motion and a constant velocity close to 3.2 m/s can be found by the simulation.

Although a coarse mesh of the projectile is used, which is unable to reproduce accurately the local buckling, the numerical approach can catch the global response of the projectile in terms of velocity and deceleration (and so in terms of total forces applied to the structure). No simulation with refine mesh for the projectile has been carried out: the aim objective of the ballistic pendulum simulation was to reproduce the projectile global response and in this way validate the load applied on the structure.

Figure 16 shows the evolution of the computed force versus time. This force is exerted by the projectile on the steel block during the impact. The force oscillations are related to the plies formation. A series of plies is developed during the projectile crushing process. The maximum of the force, about 1000 kN, is reached when the previous ply is completely done and when the buckling load initiating the formation of the next ply is obtained. During the ply formation, the load decreases a lot. Thereafter the ply formation is ended when contact conditions are established on the last ply in formation. Finally the load continues to increase until the next ply formation starts. At 4 ms, the increase of force, about 200 kN, corresponds to the crash of the second part of the projectile with a thickness of 2 mm. We can correlate this large deceleration to the loss of velocity observed on Figure 15 at 4 ms.

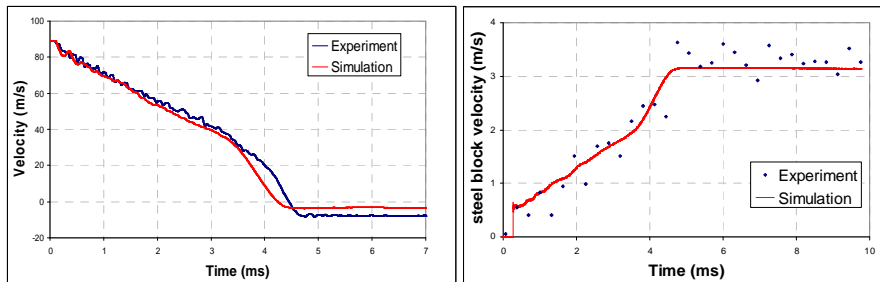


**Figure 15.** Evolutions of the projectile and pendulum velocities ( $V_0 = 89.2$  m/s)

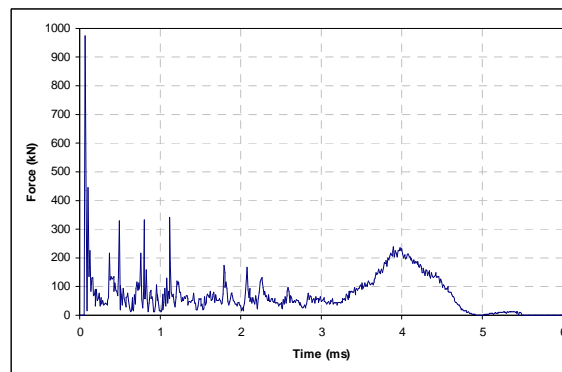
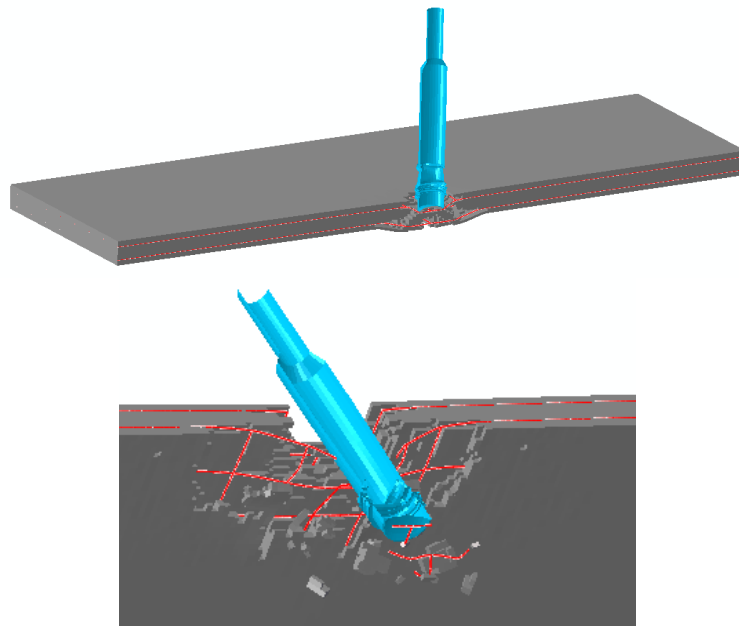


**Figure 16.** Evolution of the computed projectile impact force

### 3.3.2 Simulation of the perforation test

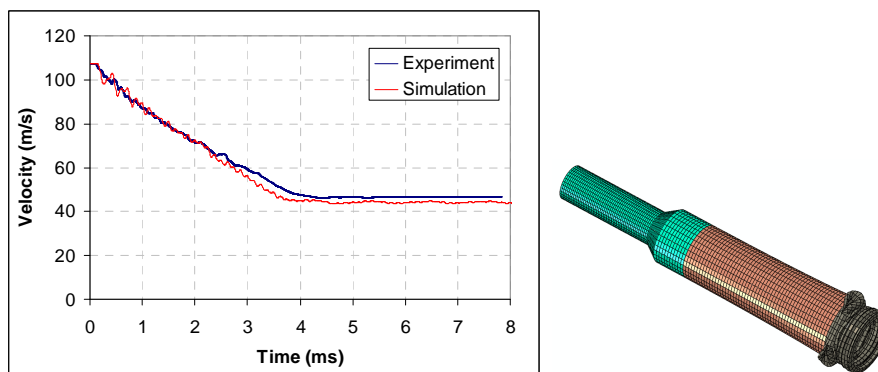
A 3-D finite element model with solid brick elements has been used for the target (60 000 eight nodes solid elements). The reinforcement is explicitly modeled using 2 nodes beam elements with a circular cross section (3 342 elements). These reinforcement elements are embedded in the concrete finite element mesh. Two symmetry planes are used and only a quarter of the plate and the projectile is modeled. Concrete nodes are not coincident with the reinforcement nodes but a displacement constraint is applied on these nodes in order to simulate a perfect link between steel and concrete. The projectile mesh and the material model are the same as those defined in the ballistic pendulum simulation.

Figure 17 shows the projectile/target interaction at 2.5 and 10 ms during the test n°1. We can observe scabbing phenomena, the formation of a concrete plugging cone and the failure of the reinforcement during the projectile penetration phase. Failure mechanisms seem to reproduce very well the experimental observations. For erosion technique, we used in PRM model an erosion criterion based on principal tensile strains developed during damage process (this criterion takes into account the strain rate effects and the hillborg method).



**Figure 17.** Numerical simulation results obtained at 2.5 ms and at 10 ms (test n°1,  $V_0 = 107.5$  m/s)

On Figure 18, the projectile velocity obtained during the test (calculated by integration of the accelerometer signal) is compared to the numerical velocity. The simulated velocity profile matches accurately the experimental data, especially the residual velocity at the end of the perforation process. On this figure, we can also observe the residual projectile shape that can be compared to the experimental residual shape shown in Figure 3 (the first cylinder part with a thin wall thickness of 1 mm is completely buckled).



**Figure 18.** Evolution of the projectile velocity and residual projectile shape (test n°1,  $V_0 = 107.5$  m/s)

To verify the independance of numerical solutions to the mesh size, we have increased the element's number by a factor of 2 in all directions on the concrete slab (480 000 eight nodes solid elements). The Figure 19 compares projectile velocity evolution during impact obtained with a coarse mesh (a) and a fine mesh (b). A good agreement is observed despite the large difference between the mesh sizes.

Figure 20 presentz projectile/target interaction at 5 ms after impact. Same local deformation on projectile and slab can be observed with both mesh sizes. Cratering and scabbing seem to develop similarly on concrete structure. CPU time is about 20 minutes for coarse mesh and 3 h 21 min for fine mesh (simulations performed on 8 SGI processors).

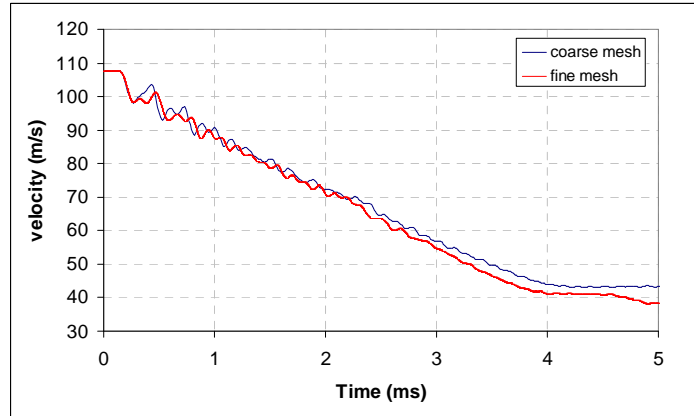


**Figure 19.** Evolution of the projectile velocity for 2 mesh sizes

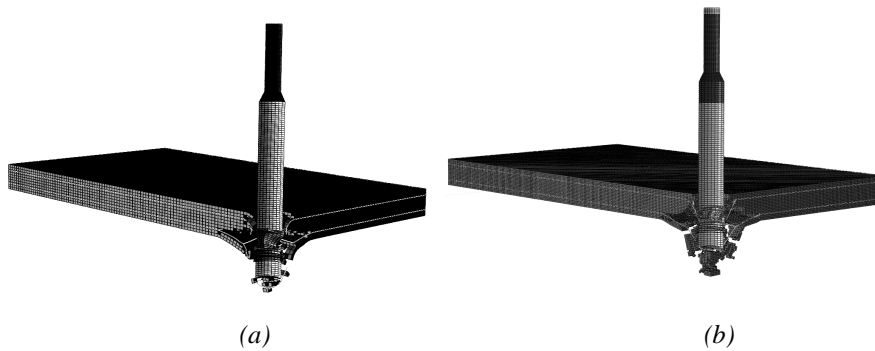


**Figure 20.** Numerical result for coarse mesh (a) and fine mesh (b) at 5 ms (test n°1,  $V_0 = 107.5$  m/s)

### 3.3.3 Simulation of the non perforating test

Material data used in the previous simulations is also used here. On Figure 21, we compare the numerical and the measured projectile velocities obtained in test n°2. The numerical simulation is able to reproduce the missile deceleration and the rebound at the end of the impact process. On this figure, we observe also the projectile shape at the end of the numerical simulation (to be compare to Figure 5). The first cylinder part with a thin wall thickness of 1 mm is buckled in both figures over a length of about 150 mm.

Figure 22 shows the computed damage pattern shape observed on the front and the rear faces and through the thickness of the target at the end of the numerical simulation (at 200 ms). The contours plotted on the reinforced concrete target give the maximum values reached by the principal tensile strains. The blue contour

corresponds to yielded rebar. This means that residual open cracks are visible on the blue part but not on the grey part. Numerical results show that the reinforcement doesn't fail (reinforcement maximum tensile strains remain below 5 % everywhere in the reinforced concrete plate) but formation of a plugging cone is initiated on the rear face of the reinforced concrete plate (like in the experiment – see Figure 6).

Figure 23 shows the displacement histories of the two points DV2 and DV4 located on the rear face of the reinforced concrete plate. A good agreement is observed between experiment and simulation concerning the maximum displacements but damping is undervalued in the computation. Perhaps frictional forces between the reinforced concrete slab and the supports explain such phenomena.

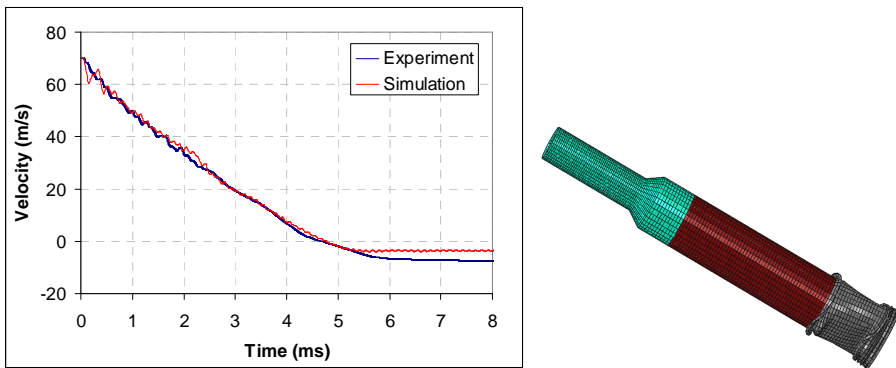


**Figure 21.** Evolution of the projectile velocity and projectile shape (test n°2,  $V_0 = 70.2$  m/s)

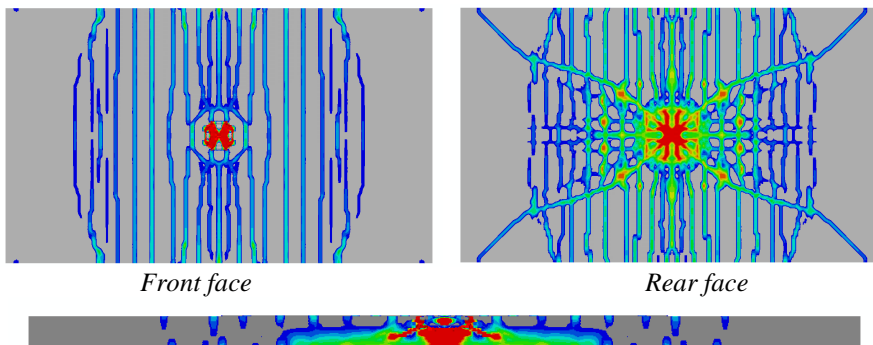


**Figure 22.** View of the maximum principal tensile strains reached on the reinforced concrete target during the impact (test n°2,  $V_0 = 70.2$  m/s)

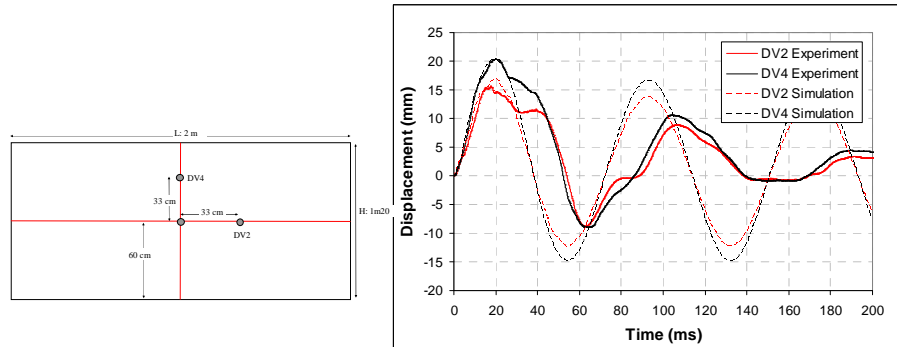


**Figure 23.** Measured and computed displacements at point DV2 and DV4 (test n°2,  $V_0 = 70.2$  m/s)

#### 4. Conclusions

An experimental and modeling approach of soft projectile impact on thin slabs presented in this paper demonstrates the efficiency of the proposed explicit finite element procedure to capture the real behavior of the reinforced concrete structure and projectile.

New soft projectile impact experiments completed by material characterizations in static and dynamic loadings provide a relevant experimental database to carry out numerical simulations and validate the modeling approach. Ballistic Pendulum test allows to validate projectile model before to simulate the complex projectile/target interaction.

The numerical results show the capabilities of the PRM model for concrete and Johnson Cook dynamic failure model for steel rebar to reproduce accurately the bending response of the reinforced concrete slab and the concrete failure mode due to the projectile impact (displacements - damaged areas, crack pattern, plugging and scabbing damage modes of the reinforced concrete slab - velocity and residual shape of the projectile).

A damage model with irreversible strains and strain rate effects in tension seems relevant to correctly catch the different mechanisms occurred on concrete. Due to damage localization process, this model has to be coupled to a regularization method to limit mesh size effects on structural response.

Using Johnson Cook dynamic failure model for steel reinforcement allows to reproduce strain rate effects on material strength but especially on ductility.

This modeling approach can advantageously help to predict the vulnerability of reinforced concrete structures to impact problems.

### Acknowledgements

This concrete program research has been performed with the financial support of the French ministry of defense (DGA). The French Agency (ANR PGCU 2007) and 3SR Laboratory at Grenoble are also gratefully acknowledged.

### References

- Baroth J., Daudeville L., Malécot Y., « About empirical models predicting the missile perforation of concrete barriers », *European J. of Environmental and Civil Engrg*, 2011 (to appear).
- Erzar B., Forquin P., Buzaud E., Pontiroli C., « Tensile strength of mortar over a wide range of strain rate », *DYMAT2009*, Bruxelles, Proceedings.
- Gabet T., Malécot Y., Daudeville L., « Triaxial behavior of concrete under high stresses: Influence of the loading path on compaction and limit states », *Cement and Concrete Research*, 38 (3), 2008, p. 403-412.
- Hillerborg A., Modeer M., Petersson P. E., « Analysis of crack formation and growth in concrete beams of fracture mechanics and finite elements », *Cement and Concrete Research*, 1976, vol. 6, p. 773-782.
- Johnson G. R. and Cook W. H., « Fracture characteristics of three metals subjected to various strains, strain rates, Temperatures and pressures », *Engineering Fracture Mechanics*, 1985, vol. 21, n° 1, p. 31-48.
- Jonas W., Rüdiger E., Gries M., Riech H., Rützel H., Kinetische Grenztragfähigkeit von Stahlbetonplatten, RS 165, Schlussbericht (Rapport final), IV. Technischer Bericht, Hochtief AG, 1982.
- Mazars J., « Application de la mécanique de l'endommagement au comportement non-linéaire et à la rupture du béton de structure ». Thèse d'état de l'Université Paris VI, France, 1984
- Pontiroli C., Rouquand A., Mazars J., « Predicting concrete behaviour from quasi-static loading to hypervelocity impact. An overview of the PRM Model », *European Journal of Environmental and Civil Engineering*, 2010, vol. 14/6-7, pp. 703-727 – doi :10.3166/ejece.14.703-727.
- Riech H., Rüdiger E., Versuchsergebnisse des Meppener Versuche II/11 bis II/2 (Results on MEPPEN tests II/11 to II/22), Technischer Bericht 1500 408 (RS 467), 1984.
- Rouquand A., IRIS 2010 International Benchmark, Impact of soft projectiles on a reinforced concrete plate: presentation of the CEA-Gramat results, CEA-Gramat, Technical Report 2010.
- Saarenheimo A., Tuomala M., Hakola I., Hyvärinen J., Aalto A. and Myllymäki J., « Impacts of deformable missiles on reinforced concrete walls », *CONSEC'07*, 2007, Tours, France.
- Vu X.H., Malecot Y., Daudeville L., Buzaud E., « Experimental analysis of concrete behavior under high confinement: Effect of the saturation ratio », *International Journal of Solids and Structures*, 2008, doi: 10.1016/j.ijsolstr.2008.10.015.